



## Diffusion brazing of Ti–6Al–4V and AISI 304: an EBSD study and mechanical properties

Ehsan Norouzi<sup>1,\*</sup>, Morteza Shamanian<sup>1</sup>, Masoud Atapour<sup>1,\*</sup>, and Babak Khosravi<sup>2</sup>

<sup>1</sup>Department of Materials Engineering, Isfahan University of Technology, Isfahan 84156-83111, Iran

<sup>2</sup>Department of Materials Science and Engineering, Sharif University of Technology, P.O. Box 11155–9466, Tehran, Iran

Received: 24 April 2017

Accepted: 8 July 2017

Published online:

17 July 2017

© Springer Science+Business Media, LLC 2017

### ABSTRACT

Ti–6Al–4V and AISI 304 stainless steel were joined by diffusion brazing with a Cu interlayer at 900 °C for different bonding times. The influence of the bonding time on the joint width, microstructure, microhardness and shear strength was studied. Interfacial characterizations and the identification of phases were done by scanning electron microscopy and electron backscatter diffraction (EBSD). The results revealed that by increasing the bonding time, the thickness of the joint was first increased and then decreased. Microstructure examinations also showed that the joints consisted of several intermetallics such as TiCu, Ti<sub>2</sub>Cu, TiCu<sub>4</sub>, TiCu<sub>2</sub>, FeTi and Fe<sub>2</sub>Ti. On the other hand, EBSD results demonstrated that the density of Cu–Ti intermetallics was reduced with the prolonged bonding time of 80 min, thereby indicating the occurrence of isothermal solidification. The microhardness profiles also showed a different behavior with varying the bonding time due to the change in the mechanism of the joint formation. The maximum shear strength obtained was 247 MPa, when the joint was bonded for 80 min; this was approximately equal to the stainless steel strength.

### Introduction

Ti–6Al–4V alloy is one of the most renowned Ti-based alloys categorized in the group of  $\alpha/\beta$  alloys. Suitable physical properties, high strength-to-weight ratio and superior corrosion resistant behavior have made this alloy a good candidate in areas such as biomaterials, marine technologies and aerospace [1, 2]. The 304 austenitic stainless steel is a conventional alloy in the group of stainless steels with applications in various industries because of its

corrosion resistance behavior in approximately all environments [3, 4].

Nowadays, joining the Ti-based alloys to the 304 stainless steel has numerous applications in chemical, military and aerospace industries due to their premiere mechanical properties and corrosion resistance [5, 6]. Fusion welding accompanied by melting can result in the appearance of big  $\beta$ -phase grains, leading to some solidification cracking that deteriorates the quality of the final product [7, 8]. Previously, various solid-state methods have been applied for

Address correspondence to E-mail: e.norouzi@ma.iut.ac.ir; m.atapour@cc.iut.ac.ir

this purpose. Kumar et al. [9] reported the friction welding of Ti–6Al–4V to 304 AISI austenite stainless steel. Their study showed that utilization of copper as the interlayer made a high strength, as compared to the joints prepared without the interlayer. Electron beam welding was successfully used for joining titanium alloy to the stainless steel via the copper interlayer by Tomashchuk et al. [10]. They concluded that the addition of copper led to a reduction in the formation of Ti–Fe and Ti–Cr brittle phases. Mousavi et al. [11] studied the explosive welding of Cp–Ti to the 304 stainless steel. The results revealed that numerous intermetallic compounds such as Fe<sub>2</sub>Ti and Fe<sub>2</sub>TiO<sub>4</sub> were formed in the interface. Liu et al. [12] also discussed the brazing of Ti–6Al–4V and the 304 AISI. Their study showed that at the Ti alloy/interlayer interface, the brittle intermetallics tended to form. Ozdemir et al. [13] reported the diffusion bonding of Ti–6Al–4V to AISI 304 by inserting a Cu interlayer (60 μm). The maximum shear strength of 118 MPa was obtained in the specimen joined at 870 °C.

Diffusion brazing is a solid-state joining process suitable for the aforementioned alloys; it has, in fact, the least influence on the microstructure of these alloys in conjunction with applying a well-made connection. Diffusion brazing is also named transient liquid-phase (TLP) bonding [14]. TLP is a combination of diffusion bonding and the brazing process. To perform a TLP bonding, an initial interlayer is placed between two base materials, and all of the components are subjected to heat at the joining temperature for a specific time. This specific temperature is a few degrees above the melting point of the interlayer. Placement of this system at high temperature leads to the cross-diffusion of each side into each other. Thus, the melting point of the created alloying system is increased, leading to the occurrence of isothermal solidification and the decrement in joint width until the completion of solidification. In this regard, TLP is divided into three major groups including dissolution of the interlayer, homogenization of the liquid and isothermal solidification [15]. Lately, researchers have conducted some studies on the TLP of Ti-based

and stainless steels. Deng et al. [16] reported the TLP bonding of Ti–6Al–4V using a pure copper interlayer at 930 °C. It was revealed that the optimized joint was achieved in 30 min; moreover, a maximum tensile strength value of 944 MPa was recorded for the bonds. Recently, the effect of the bonding temperature on the TLP bond of Ti–6Al–4V and SS 304 was investigated by our group [17]. It was found that by raising the bonding temperature, the amount of the brittle compounds was reduced gradually and the highest shear strength of 374 MPa was obtained at 960 °C.

The purpose of this research paper was to investigate the effect of the bonding time on the diffusion brazing of Ti–6Al–4V and the 304 stainless steel and evaluate the microstructural and mechanical characteristics. The innovation of this paper, as compared to other similar studies, has been accurate identification and distribution of various phases in the joint area by using electron backscatter diffraction (EBSD).

## Experimental

The materials used in this study were Ti–6Al–4V and AISI 304 with the dimensions of 40 mm × 10 mm × 3 mm. Their compositions in weight percent are given in Table 1. The bonding was carried out using Cu (25 μm) as the interlayer. All samples were ground using progressively finer SiC paper through 1200 grit and then polished. The specimens and the interlayer were subsequently degreased in an ultrasonic bath. The process was performed in a furnace under the vacuum of  $3 \times 10^{-3}$  Pa for the bonding time of 20, 40, 60 and 80 min at 900 °C. After bonding, interface microstructures were characterized by optical microscopy (OM) and scanning electron microscopy (SEM). A Hitachi SU8230 field emission scanning electron microscope (FE-SEM) was used for energy-dispersive spectrometry (EDS) and electron backscattered diffraction (EBSD) analysis of the bonded zones for 40 and 80 min. The analysis of EBSD maps and identification of intermetallic were

**Table 1** Chemical composition (wt%) of the base metals

Materials	Fe	Ti	Cr	Al	V	Ni	Si	O	C	Mn	Cu	Other
304SS	Base	–	19.2	–	0.06	9.5	0.6	–	0.08	1.2	0.3	<0.2
Ti–6Al–4V	0.14	Base	0.01	5.8	3.9	0.01	0.04	–	0.01	0	–	<0.2

carried out by EBSD channel 5 software. The strength of the joints was determined using a shear test fixture with a crosshead speed of 1 mm/min. A shear test jig was developed to hold the bonded samples during shear testing, as presented schematically in Fig. 1. An average of three samples was taken for each shear strength reported. Microhardness was measured across the bond interface using a load of 50 g.

## Results and discussion

### Microstructure characterization

Figure 2a–d represents the microstructure of the specimens bonded at different holding times of 20, 40, 60 and 80 min. As shown in Fig. 2a, at the bonding time of 20 min, the copper interlayer started

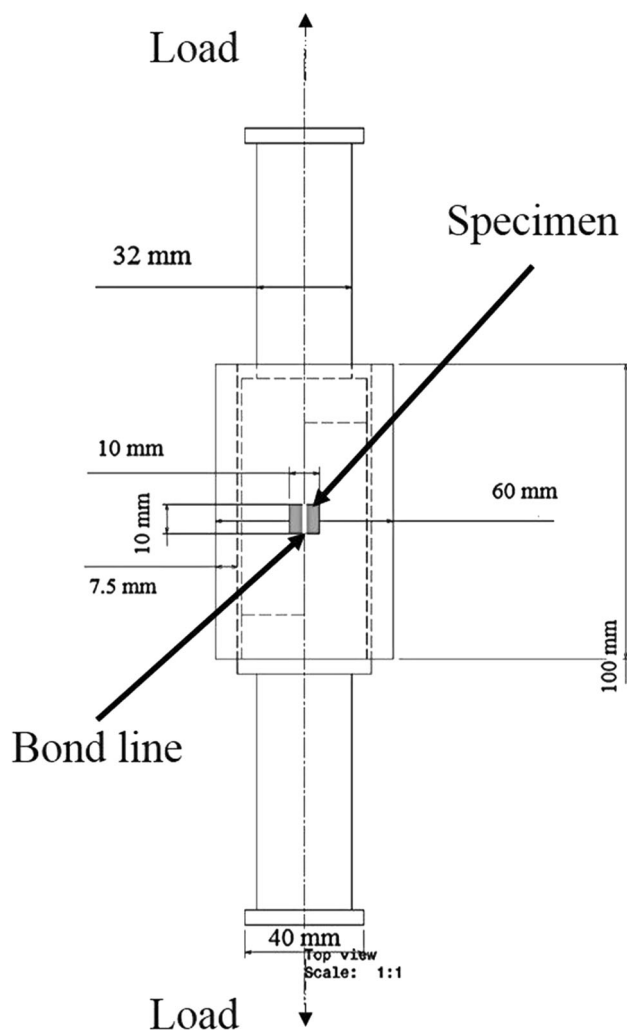


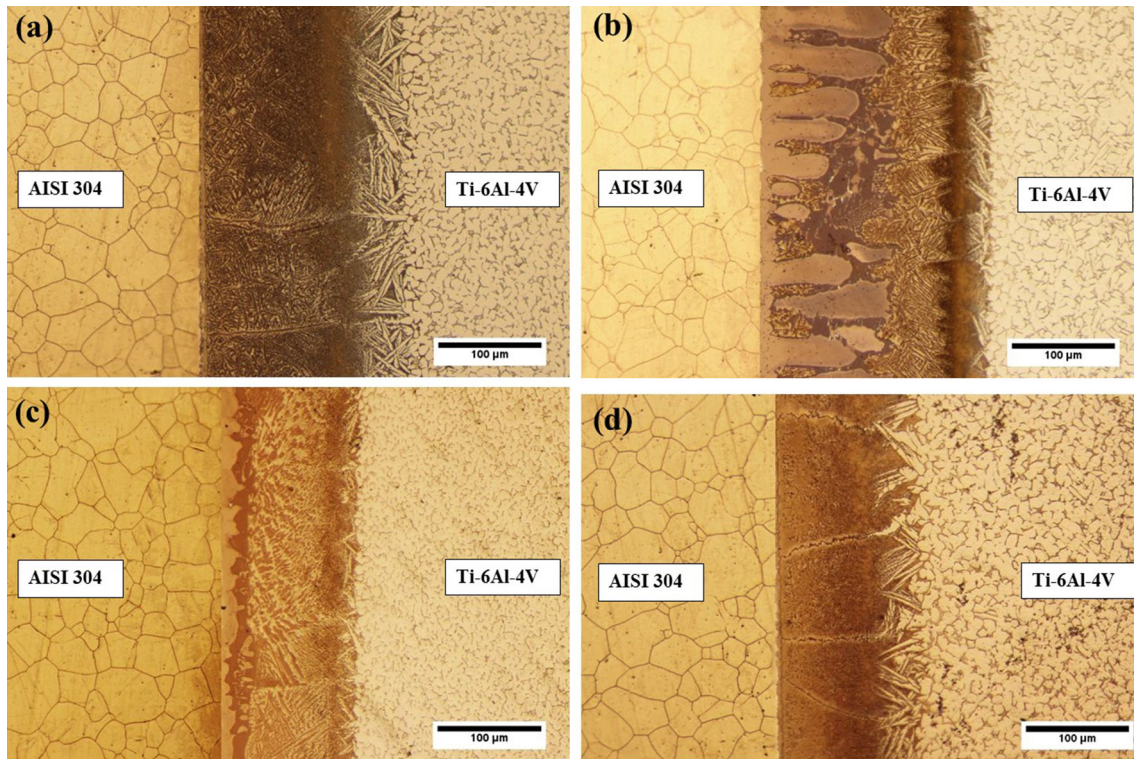
**Figure 1** A schematic to show shear test.

to dissolve, producing a large amount of the eutectic liquid inside joint zone, according to the Cu–Ti phase diagram. Since the temperature of the Cu–Ti eutectic was about 870 °C, by elevating the bonding temperature to 900 °C (above the eutectic point), base metals dissolution began due to the diffusion of Cu from the liquid into the solid substrate. Widening of the liquid phase occurred with a prolonged bonding time from 20 to 40 min. The liquid zone continued to widen, producing a maximum gap width during the process. Increasing the bonding time from 40 to 60 min led to changing the joint morphology. It could be due to more diffusion of elements at the interface. This phenomenon caused the shrinkage of the liquid width via isothermal solidification. The reduction in the joint thickness to 133 μm could be attributed to onset isothermal solidification. Further increasing the holding time to 80 min resulted in a slight decrease in the joint width to 125 μm. As expected, it was observed that the complexity of the phases and intermetallics formed within the joint was decreased with increasing the brazing time. However, this time was not adequate for the complete isothermal solidification. Generally, the completion of isothermal solidification was controlled by the solid-state diffusion of the elements interlayer into the base metals.

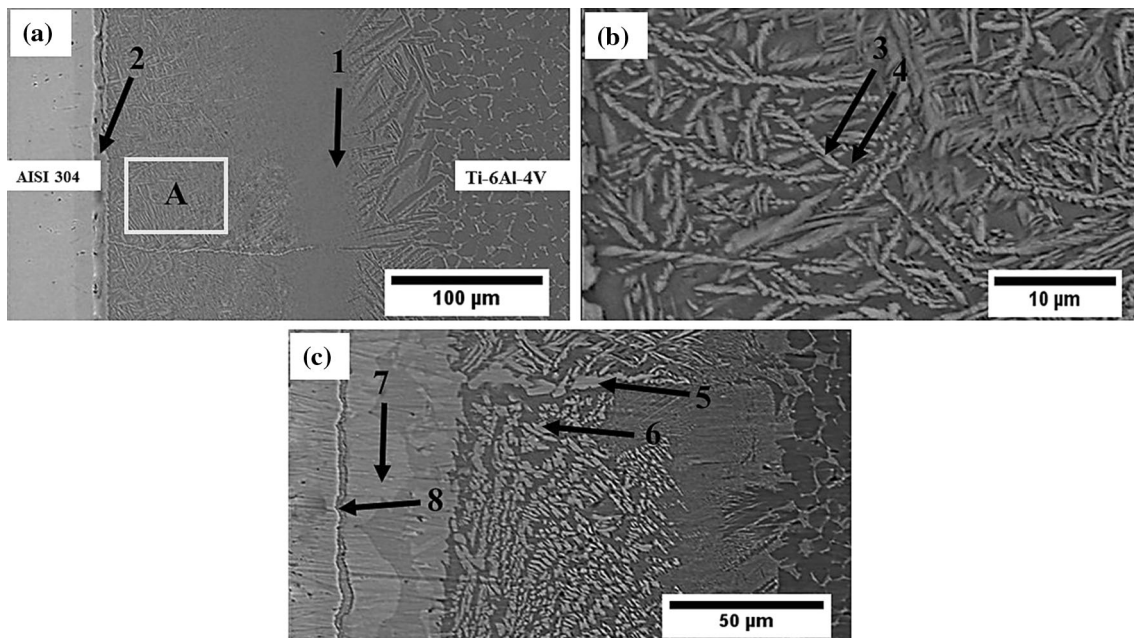
A typical micrograph of the Ti–6Al–4V/Cu/SS 304 brazed joint at 900 °C for 20 min is shown in Fig. 3. The chemical composition of each region was determined by EDS, as listed in Table 2. Intermetallic phases were formed in the region zone. EDS analysis verified that the phase marked 1 was TiCu, according to the Cu–Ti phase diagram (Fig. 4). The region 2, which was adjacent to the AISI 304, detected a significant amount of iron and titanium. This suggested that it was Fe<sub>2</sub>Ti. Several studies have also reported the same observation [18, 19]. The higher magnification figure of the joint is presented in Fig. 3b. The chemical composition of the point 3 showed that the weight ratio of Ti to Cu was about 2:1, thereby confirming the possible formation of Ti<sub>2</sub>Cu. The region 4 contained high Ti concentration, which was predicted to be α-Ti.

Figure 3c illustrates the interfacial microstructure joint brazed for 60 min. EDS compositional analysis in zones 5 and 6 could lead to deducing TiCu<sub>2</sub> and TiCu<sub>4</sub>, respectively. It was demonstrated that the presence of these phases could be due to the eutectic reaction between Cu and Ti:  $L \rightarrow \text{TiCu}_2 + \text{TiCu}_4$ ; similar results have also been obtained in the literature [17, 20]. The diffusion of Fe and Ti from the base





**Figure 2** Microstructure of the joints bonded at 900 °C for: **a** 20 min, **b** 40 min, **c** 60 min and **d** 80 min.



**Figure 3** SEM micrographs of the interface for bonds produced at a bonding time of: **a** 20 min, **b** magnified image of area A and **c** 60 min.

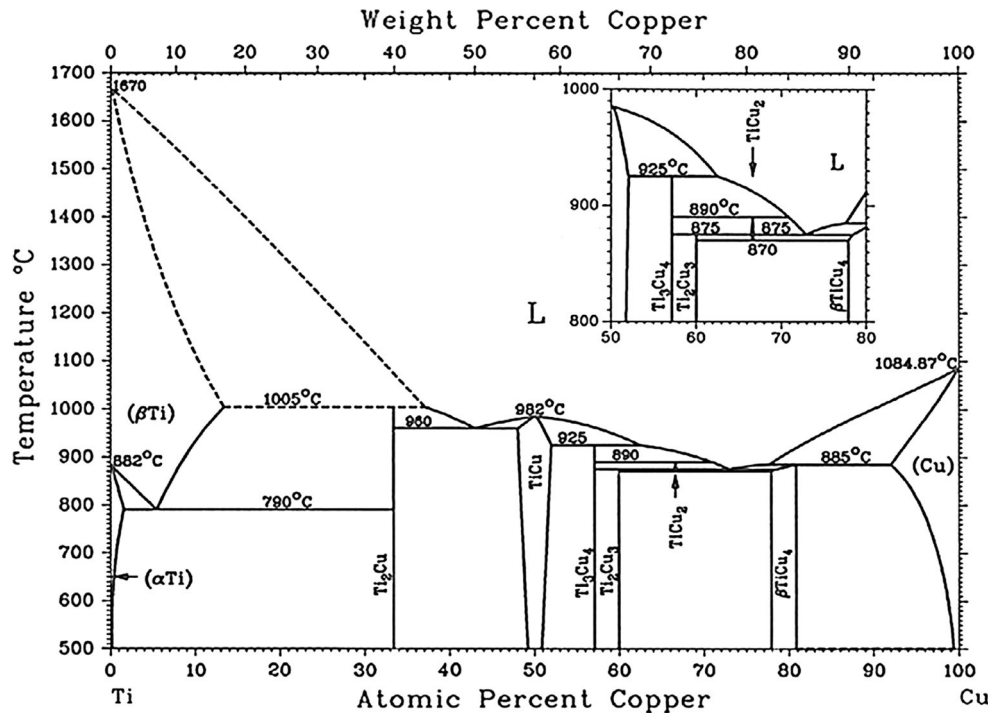
metals due to the concentration gradient resulted in the formation of FeTi and Fe<sub>2</sub>Ti at the joint region (marked as 7 and 8).

The microstructure and phase distribution of the joint for 40 min are presented in Fig. 5a, b, respectively. It could be seen that a number of compounds

**Table 2** EDS analysis results for the different regions in Fig. 3, wt%

Region	Ti	Cu	Fe	Al	V	Cr	Ni	Deduced phases
1	47.8	45.4	1.3	2.7	1.2	0.9	0.7	TiCu
2	30.7	4.8	54.2	0	0	5.9	4.4	Fe <sub>2</sub> Ti
3	68.7	22.4	2.3	1.2	0.8	1.7	2.9	Ti <sub>2</sub> Cu
4	78.3	15.1	2.1	0.8	0.4	1.1	2.2	α-Ti
5	30.4	66.9	0.4	1.1	0	1.2	0	TiCu <sub>2</sub>
6	20.3	72.4	0.8	1.5	0.8	3.1	1.1	TiCu <sub>4</sub>
7	29.4	3.8	58.4	0.8	0.3	4.6	2.7	FeTi
8	27.1	2.6	61.7	0	0	5.5	3.1	Fe <sub>2</sub> Ti

**Figure 4** Ti–Cu binary alloy phase diagram.



consisting of Ti<sub>2</sub>Cu, TiCu, FeTi and Fe<sub>2</sub>Ti were determined with different colors. It was found that a mixture of Ti<sub>2</sub>Cu with α-Ti could be produced through the eutectoid reaction (β-Ti → α-Ti + Ti<sub>2</sub>Cu), as also reported by other researchers [16, 17]. As shown, the presence of Cu–Ti compounds was much more than that of the Fe–Ti intermetallic at the joint zone; this was due to the fact that the diffusion rate of the Ti in Cu is so high [21]. Figure 5c shows the EBSD orientation map of the joint, where the various colors could reveal different orientations of the grains. The legend for inverse pole figure (IPF) from the formed phases is presented in Fig. 5d. The micrograph and the EBSD phase distribution diagram of the brazed joint at 80 min are shown in Fig. 6a, b. It could be seen that TiCu, FeTi and Fe<sub>2</sub>Ti were produced at the

joint. The EDS point analysis of the Ti–6Al–4V/AISI 304 joint interface for the bonding times of 40 and 80 min is given in Table 3. It was observed that the EDS analysis confirmed the presence of these compounds in the bonded area. At the high temperature, a significant amount of titanium could be dissolved in α-Fe and the same thing could happen in β-Ti. However, at the low temperature (under 400 °C), the solubility between Fe and Ti was poor. Therefore, it was responsible for the formation of intermetallic compounds such as FeTi and Fe<sub>2</sub>Ti at the ambient temperature. It was also noticed that the formation of Cu–Ti phases was decreased significantly when compared with samples bonded at the lower times. This could be ascribed to the increment in isothermal solidification rate by increasing the bonding time.



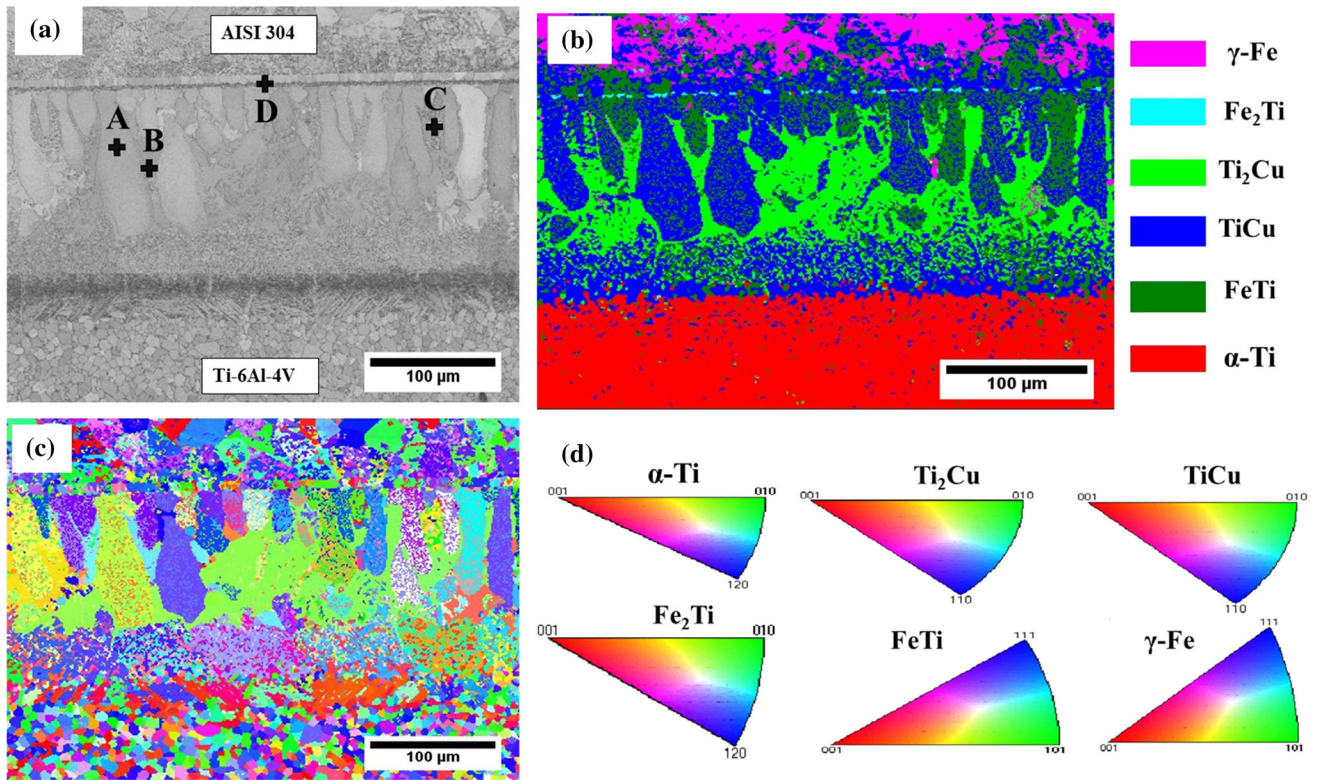


**Figure 5** EBSD-SEM micrographs of sample bonded for 40 min at 900 °C. **a** IQ map, **b** phase map, **c** IPF map and **d** legend of IPF map.

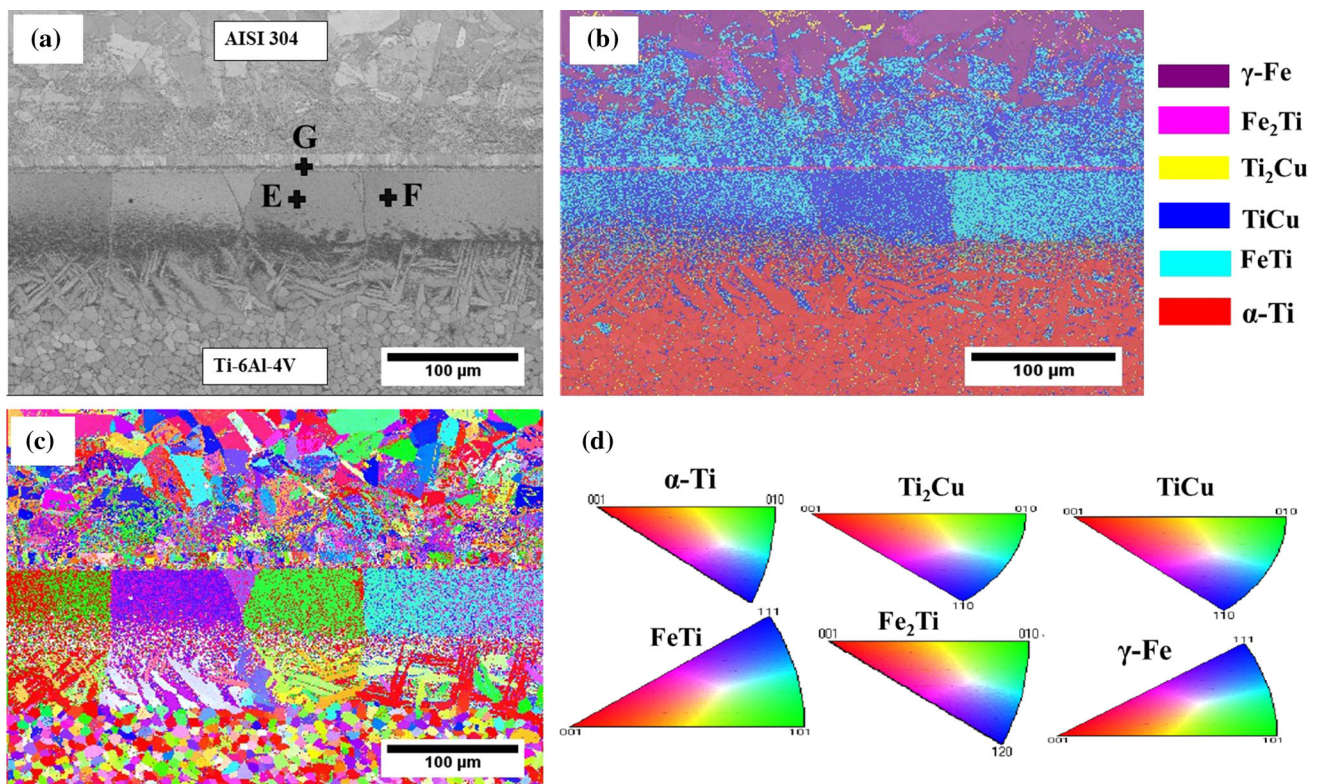
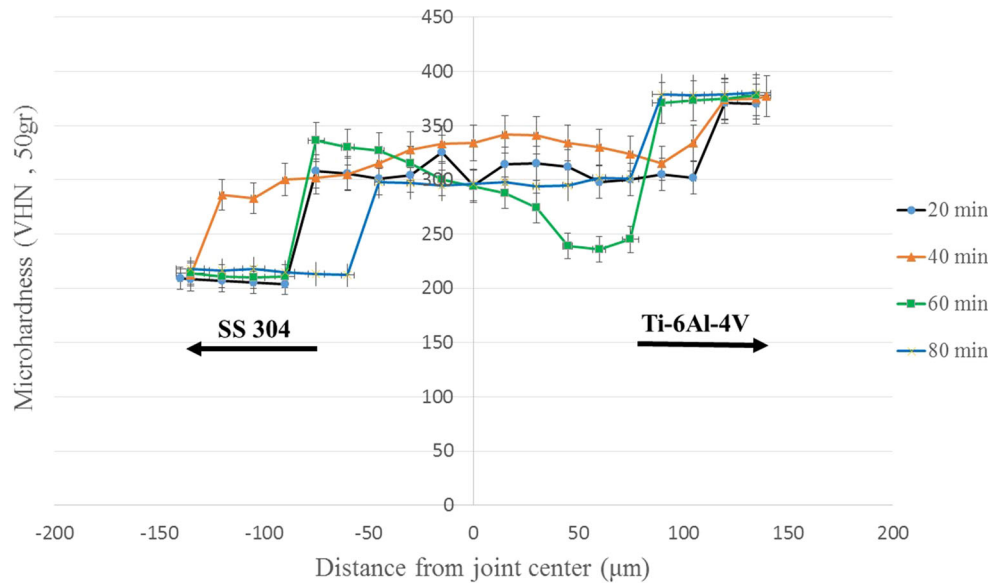


**Figure 6** EBSD-SEM micrographs of sample bonded for 80 min at 900 °C. **a** IQ map, **b** phase map, **c** IPF map and **d** legend of IPF map.

**Table 3** EDS analysis (wt%) of selected regions for the bonds shown in Figs. 5, 6

Region	Ti	Cu	Fe	Al	V	Cr	Ni	Suggested phases
A	45.2	40.1	7.1	1.5	1.4	2.6	2.1	TiCu
B	56.4	27.2	4.2	1.7	0.9	5.1	4.5	Ti <sub>2</sub> Cu
C	27.4	2.1	60.4	1.3	0.6	7.1	1.1	FeTi
D	25.3	1.3	61.8	0.6	0.2	8.4	2.4	Fe <sub>2</sub> Ti
E	41.7	34.9	19.1	1.1	0.6	1.8	0.8	TiCu
F	22.3	10.2	54.8	1.1	0.4	6.1	5.1	FeTi
G	16.1	2.8	63.7	0.7	0.4	9.6	6.7	Fe <sub>2</sub> Ti

**Figure 7** Microhardness profile across the joints made at 900 °C for different bonding times.



Evidently, with increasing the brazing time, the quantity of intermetallic compounds was reduced. In the present study, it was well demonstrated that EBSD provided important information about the accuracy of distribution phases in the joint zone. Moreover, it was found that a narrower joint zone was achieved in comparison to the previous similar studies.

**Mechanical properties of the joint**

Figure 7 represents the microhardness profile for different joints made at 900 °C. It could be seen that the microhardness profile for the bond made at 20 min gave a hardness value of 296 VHN at the joint center. Average hardness indicated that the couple bonded at the bonding time of 40 min had the maximum value inside the joint zone with 342 VHN. It could be attributed to the high density of intermetallics at the center joint. The hardness at the bond center was increased with the bonding time owing to

the diffusion of titanium and iron into the joint center and the diffusion away of copper from the center line, leading to the formation of Ti–Fe compounds. In other words, for a short bonding time, the joint center was rich in Cu, resulting in lower hardness across the joint zone. For a holding time of 60 min, at a distance of 30 µm from the joint center and on the titanium side, the profile showed the minimum hardness value of 236 VHN across the joint region; on the other hand, this was recorded to be 342 VHN at a distance of 70 µm from the center line for a bonding time a 40 min. When the bonding time was increased to 80 min, the profile revealed uniform hardness across both Ti–6Al–4V and AISI 304, as compared to prior samples. The gradual homogenization of the joint and the change in the formation of brittle compounds at the interface could be responsible for the differences in microhardness profiles. Evidently, hardness values were affected by grain size; the average grain size of the base metals for different bonds is presented in Table 4. It was observed that raising the



bonding time led to a continuous reduction in the hardness of the base metals due to the grain growth that occurred, according to the Hall–Petch equation.

The interfacial bond strength of the joints was performed by the single lap shear test with varying bonding time. The results are displayed in Fig. 8. The joint fabricated for 20 min recorded the shear strength of 164 MPa. Increasing the bonding time from 20 to 40 min resulted in the deterioration of shear strength, reaching to 139 MPa, which was the minimum value of the strength in the present work. This could be due to the fact that the width of the joint is increased with the rise of the holding time. Prolonged bonding time led to widening the liquid at the interface, as a result the deteriorated shear strength. This observation is consistent with reports in the literature [16, 19]. The strength was increased with further increasing the bonding time from 40 to 60 min, reaching to 195 MPa. As discussed earlier, the width of joint was reduced, leading to the better joint strength. The maximum strength was 247 MPa of the bond made for 80 min, which was approximately equal to the strength of the stainless steel. This could be correlated with the lower density of Cu–Ti phases inside the joint and an increment in the rate of isothermal solidification, leading to the higher mechanical properties. The metallurgical

combination and microstructure could remarkably affect the shear strength of the joints. The considerable interdiffusion of Cu, Ti and Fe across joint zone indicated that the formation of Cu–Ti and Fe–Ti was inevitable at the interface. On the other hand, it has been well demonstrated that Cu–Ti and Fe–Ti compounds have a tendency to embrittle the bond [16, 20, 22]. It was clear that the mechanical properties could be improved by reduction in these phases within the joint. In the present work, firstly, the amount of eutectic and intermetallic phases was increased and then decreased as the bonding time was increased. Hence, it could be concluded that the strength should be increased by elevating the bonding time. The observed results for the shear strength were in a good agreement with those mentioned above.

## Summary and conclusions

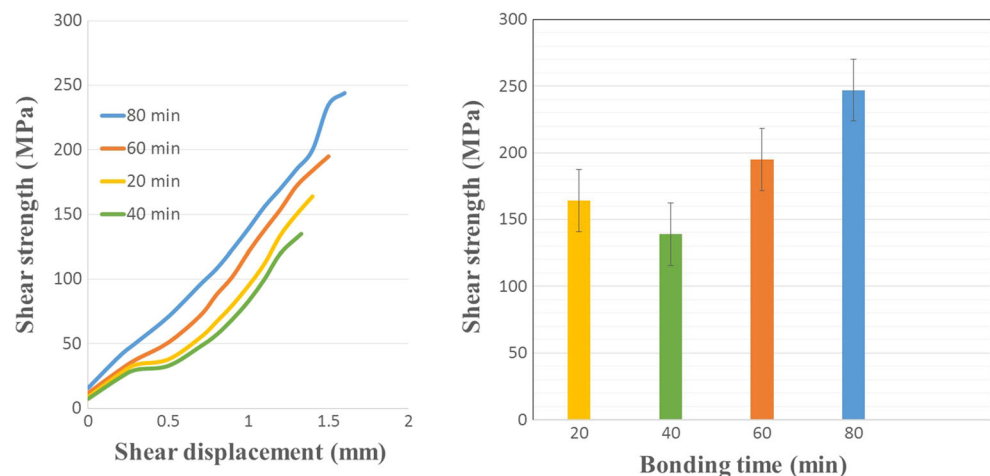
The effect of the bonding time on diffusion brazing of Ti–6Al–4V/Cu/SS 304 was investigated. The major findings and conclusions are drawn here:

- (1) The interface characterization showed that by elevating the bonding time, the joint width was first increased and then continued to be decreased, indicating the occurrence of the isothermal solidification.
- (2) The SEM–EDS and EBSD phase mapping revealed that the interdiffusion of Ti, Fe and Cu led to the formation of TiCu, Ti<sub>2</sub>Cu, TiCu<sub>4</sub>, TiCu<sub>2</sub>, FeTi and Fe<sub>2</sub>Ti, producing a metallurgical bond at the interface.

**Table 4** Average grain size ( $\mu\text{m}$ ) of the base metals for different brazing times

Bonding time (min)	20	40	60	80
304SS	23.1	26.1	28.4	30.2
Ti–6Al–4V	8.4	10.1	11.6	13.7

**Figure 8** Shear strength as a function of bonding time for the joints fabricated at 900 °C.





- (3) EBSD-SEM also confirmed that the Cu–Ti intermetallics density was reduced for a prolonged bonding time of 80 min, thereby implying the occurrence of the isothermal solidification.
- (4) The highest value of shear strength obtained was 247 MPa, which was approximately equal to the strength of AISI 304.

### Compliance with ethical standards

**Conflict of interest** The authors declare that they have no conflict of interest.

### References

- [1] Atasoy E, Kahraman N (2008) Diffusion bonding of commercially pure titanium to low carbon steel using a silver interlayer. *Mater Charact* 59:1481–1490
- [2] Leyens C, Peters M (2003) Titanium and titanium alloys. Wiley Online Library
- [3] Jiménez-Come M, Turias I, Trujillo F (2014) An automatic pitting corrosion detection approach for 316L stainless steel. *Mater Des* 56:642–648
- [4] Lo KH, Shek CH, Lai J (2009) Recent developments in stainless steels. *Mater Sci Eng: R: Rep* 65:39–104
- [5] Fuji A, Ameyama K, North T (1996) Improved mechanical properties in dissimilar Ti-AISI 304L joints. *J Mater Sci* 31:819–827. doi:10.1007/BF00367903
- [6] Serhan H, Slivka M, Albert T, Kwak SD (2004) Is galvanic corrosion between titanium alloy and stainless steel spinal implants a clinical concern? *Spine J* 4:379–387
- [7] Atabaki MM (2010) Microstructural evolution in the partial transient liquid phase diffusion bonding of Zircaloy-4 to stainless steel 321 using active titanium filler metal. *J Nucl Mater* 406:330–344
- [8] Williams JC, Belov A (1982) Titanium and titanium alloys: Scientific and technological aspects, vol 1. Plenum Press, New York
- [9] Kumar R, Balasubramanian M (2015) Experimental investigation of Ti–6Al–4V titanium alloy and 304L stainless steel friction welded with copper interlayer. *Def Technol* 11:65–75
- [10] Tomashchuk I, Sallamand P, Andrzejewski H, Grevey D (2011) The formation of intermetallics in dissimilar Ti6Al4V/copper/AISI 316 L electron beam and Nd: YAG laser joints. *Intermetallics* 19:1466–1473
- [11] Mousavi SA, Sartangi PF (2009) Experimental investigation of explosive welding of cp-titanium/AISI 304 stainless steel. *Mater Des* 30:459–468
- [12] Liu C, Ou C, Shiue R (2002) The microstructural observation and wettability study of brazing Ti–6Al–4V and 304 stainless steel using three braze alloys. *J Mater Sci* 37:2225–2235. doi:10.1023/A:1015356930476
- [13] Özdemir N, Bilgin B (2009) Interfacial properties of diffusion bonded Ti–6Al–4V to AISI 304 stainless steel by inserting a Cu interlayer. *Int J Adv Manuf Technol* 41:519–526
- [14] Ojo O, Richards N, Charturvedi M (2013) Effect of gap size and process parameters on diffusion brazing of Inconel 738. *Sci Technol Weld Join* 9(3):209–220
- [15] Cook GO III, Sorensen CD (2011) Overview of transient liquid phase and partial transient liquid phase bonding. *J Mater Sci* 46:5305–5323. doi:10.1007/s10853-011-5561-1
- [16] Deng Y, Sheng G, Wang F, Yuan X, An Q (2016) Microstructure evolution and mechanical properties of transient liquid phase bonded Ti–6Al–4V joint with copper interlayer. *Mater Des* 92:1–7
- [17] Norouzi E, Atapour M, Shamanian M, Allafchian A (2016) Effect of bonding temperature on the microstructure and mechanical properties of Ti–6Al–4V to AISI 304 transient liquid phase bonded joint. *Mater Des* 99:543–551
- [18] Ghosh M, Chatterjee S (2005) Effect of interface microstructure on the bond strength of the diffusion welded joints between titanium and stainless steel. *Mater Charact* 54:327–337
- [19] Zakipour S, Halvae A, Amadeh AA, Samavatian M, Khodabandeh A (2015) An investigation on microstructure evolution and mechanical properties during transient liquid phase bonding of stainless steel 316L to Ti–6Al–4V. *J Alloy Compd* 626:269–276
- [20] Elrefaey A, Tillmann W (2009) Evaluation of transient liquid phase bonding between titanium and steel. *Adv Eng Mater* 11:556–560
- [21] Castoldi L, Visalli G, Morin S, Ferrari P, Alberici S, Ottaviani G, Corni DF, Tonini R, Nobili C, Bersani M (2004) Copper–titanium thin film interaction. *Microelectron Eng* 76:153–159
- [22] Vigraman T, Ravindran D, Narayanasamy R (2012) Effect of phase transformation and intermetallic compounds on the microstructure and tensile strength properties of diffusion-bonded joints between Ti–6Al–4V and AISI 304L. *Mater Des* 36:714–727